Mutual Information-Based Texture Spectral Similarity Criterion

Michal Haindl(✉) and Michal Havlíček

The Institute of Information Theory and Automation of the Czech Academy of Sciences, Prague, Czechia
{haindl,havlimi2}@utia.cz
http://www.utia.cz/

Abstract. Fast novel texture spectral similarity criterion, capable of assessing spectral modeling resemblance of color and Bidirectional Texture Functions (BTF) textures, is presented. The criterion reliably compares the multi-spectral pixel values of two textures, and thus it allows to assist an optimal modeling or acquisition setup development by comparing the original data with its synthetic simulations. The suggested criterion, together with existing alternatives, is extensively tested in a long series of thousands specially designed monotonically degrading experiments moreover, successfully compared on a wide variety of color and BTF textures.

1 Introduction

A reliable mathematical criterion which would allow to an automatic assessment and mutual-similarity evaluation of two or more visual textures is important but still unsolved difficult image understanding problem. Recent validation of the state-of-the-art image and texture fidelity criteria [5] on the web-based benchmark (http://tfa.utia.cas.cz) has demonstrated that none of published criteria (CW-SSIM [24], STSIM-1, STSIM-2, STSIM-M) [27], ζ [13]) can be reliably used for this task at all.

However, the development of visually correct mathematical texture models and the estimation of their optimal parameters requires a reliable criterion for comparison of the original texture with a synthesized or reconstructed one. Such similarity metrics is also needed for spectral content-based image retrieval. Various textural features developed for texture classification applications such as Haralick's features [8], Run-Length features [4], Laws's filters [14], Gabor features [15], LBP [17], and so forth are not descriptive (except for Markovian features [6]), and thus, they can be used for identity but not a degree of similarity decisions. Furthermore, most advanced textural features are limited to mono-spectral images, which neglects color is arguably the most significant visual feature.

The psychophysical evaluations [7,22], i.e., quality assessments performed by humans, currently represent the only reliable but awkward option. The psychophysical texture similarity assessment requires strictly controlled laboratory

G. Bebis et al. (Eds.): ISVC 2019, LNCS 11844, pp. 302–314, 2019.
https://doi.org/10.1007/978-3-030-33720-9_23

conditions experiment design setup, representative and sufficient numbers of testers who are naive concerning the purpose and design of the experiment. Thus it is extremely impractical, expensive, generally demanding, and hence nontransferable into daily routine practice.

In this article, the visual textures or general images, we compare as independent sets of pixels irrespectively of their location. We will investigate this restricted problem of texture spectral similarity in the rest of the paper which is organized as follows: Sect. 2 briefly presents existing possibilities to solve the problem of image spectral composition comparison, including some criteria based on modifications of techniques developed for slightly different purposes. Section 3 explains in detail the proposed approach and Sect. 4 describes the performed criteria, validation experiments, and test data. Section 5 shows the achieved results. The conclusion summarizes the paper with a discussion and compares the proposed criterion with the existing alternatives.

2 Related Criteria

In this section, we briefly survey existing methods capable of comparing image spectral composition. The symbols $\downarrow, \uparrow$ indicate the increasing similarity direction for the corresponding criterion. Most methods deal with color images, i.e., three spectral channels only. The straightforward option is to use a three-dimensional (3-D) histogram or local histogram [25], which approximates the image color distribution. Let us denote by a_ϱ and b_ϱ the ϱ-th bin of the 3-D histogram of the images A and B respectively, where A is the template image and similarly B is the image to be compared. The range of the histogram multi-index $\varrho = [i, j, k]$ depends on a color space C in which the image is represented, e.g., in case of the standard 24-bit RGB color space, the range of all three components of the multi-index is an integer from 0 to 255.

The histogram based criteria often use the Minkowski distance:

$$\downarrow \varDelta_p H(A,B) = \left(\sum_{\varrho \in C} |a_\varrho - b_\varrho|^p \right)^{1/p} \geq 0. \tag{1}$$

either in the most intuitive the 3-D histograms difference version $p = 1$ ($\varDelta H$ also known as the block or Manhattan distance), or the Euclidean distance $p = 2$, a fractional dissimilarity $p = \frac{1}{2}$, alternatively, the maximum distance also called Chebyshev distance and known as chessboard distance $(p = \infty)$:

$$\downarrow \varDelta_\infty H(A,B) = \sum_{\varrho \in C} \max \{|a_i - b_i|, |a_j - b_j|, |a_k - b_k|\} \geq 0, \tag{2}$$

where a_i, a_j, a_k represents 1st, 2nd and 3rd components of vector a_ϱ and similarly for b_i, b_j, b_k. Let us mention that for $0 < p < 1$ so-called fractional dissimilarity, the Minkowski distance is not a metric because it violates the triangle inequality [10].

Several other possibilities for 3-D histogram comparison have been suggested, such as the histogram intersection [21]:

$$\downarrow \cap H(A,B) = 1 - \frac{\sum_{\varrho \in C} \min\{a_\varrho, b_\varrho\}}{\sum_{\varrho \in C} b_\varrho} \quad \geq 0, \tag{3}$$

the squared chord [12]:

$$\downarrow d_{sc}(A,B) = \sum_{\varrho \in C} \left(\sqrt{a_\varrho} - \sqrt{b_\varrho}\right)^2 \quad \geq 0, \tag{4}$$

the Canberra metric [12]:

$$\downarrow d_{can} = \sum_{C_0} \frac{|a_\varrho - b_\varrho|}{a_\varrho + b_\varrho} \quad \geq 0, \tag{5}$$

where $C_0 = \{\varrho : a_\varrho + b_\varrho \neq 0\} \subset C$.

The information theoretic measures can also be considered for evaluating the histogram difference. One possible option is the Kullback-Leibler divergence:

$$\downarrow KL(A,B) = \sum_{C^0} a_\varrho \log \frac{a_\varrho}{b_\varrho}, \tag{6}$$

where $C^0 = \{\varrho : a_\varrho b_\varrho \neq 0\} \subset C$ and $\log$ denotes common logarithm. Another possible option is the symmetric modification of the Kullback-Leibler divergence – a variant of the empirical Jeffrey divergence:

$$\downarrow J(A,B) = \sum_{C^0} a_\varrho \log \frac{2a_\varrho}{a_\varrho + b_\varrho} + b_\varrho \log \frac{2b_\varrho}{a_\varrho + b_\varrho} \quad \geq 0. \tag{7}$$

The Jeffrey divergence is numerically stable, symmetric and robust concerning noise and the size of histogram bins [18]. Another measure, based on χ^2 statistic was suggested in [26]:

$$\downarrow \chi^2(A,B) = \sum_{C_0} \frac{2\left(a_\varrho - \frac{a_\varrho + b_\varrho}{2}\right)^2}{a_\varrho + b_\varrho} \quad \geq 0. \tag{8}$$

The Earth Mover's Distance (EMD) or Wasserstein [19] is a method to evaluate dissimilarity between two multidimensional distributions in some feature space. It is based on the minimal cost that must be paid to transform one distribution into another where the cost for moving a single feature unit in the feature space is defined by the Euclidean distance, and the total cost is the sum of such single feature moving costs. The measure in its smoothed dual solution [1] is too time-consuming for any practical application (see Table 2).

The generalized color moments (GCM) [16] suits well to the image spectral composition comparison problem. The GCM of the $(p+q)$-th order and the $(\alpha+\beta+\gamma)$-th degree is defined as [16]:

$$\downarrow \Delta GCM_{pq}^{\alpha\beta\gamma}(A,B) = \left| \int\int_{\langle A \rangle} r_1^p r_2^q \, [Y^A_{r_1,r_2,1}]^\alpha \, [Y^A_{r_1,r_2,2}]^\beta \, [Y^A_{r_1,r_2,3}]^\gamma \, dr_1 dr_2 \right.$$
$$\left. - \int\int_{\langle B \rangle} r_1^p r_2^q \, [Y^B_{r_1,r_2,1}]^\alpha \, [Y^B_{r_1,r_2,2}]^\beta \, [Y^B_{r_1,r_2,3}]^\gamma \, dr_1 dr_2 \right| , \qquad (9)$$

where $[r_1, r_2] \in \langle A \rangle$ represents planar coordinates of the image pixel Y_r^A, $Y^A_{r_1,r_2,i}$ denotes a pixel intensity in the i-th spectral plane of the image A , similarly $Y^B_{r_1,r_2,r_3=i}$ where $[r_1, r_2] \in \langle B \rangle$. In the case of using GCM for spectral composition comparison, neither of the terms r_1^p and r_2^q is useful and therefore both might be put equal to one, using those GCMs for which $p = q = 0$ holds. Moreover, it has been observed that the best results are achieved if $\alpha = \beta = \gamma$, specifically using GCMs for $\alpha = \beta = \gamma < 4$. Thus, GCM directly compares image pixels not using their 3-D histograms like methods (1), (3)–(8), similar to the cosine-function-based dissimilarity, which computes an angle between two vectors. Both images A, B must have an identical number of pixels which is a significant drawback of this criterion. This criterion is the only one mentioned in this article suffering from this. All values of corresponding image spectral channels are arranged into vectors V_A and V_B and the difference is computed as [26]:

$$\uparrow d_{cos}(A,B) = \frac{V_A^T \cdot V_B}{\|V_A\| \, \|V_B\|} \quad \in \langle 0; 1 \rangle, \qquad (10)$$

where $\| \; \|$ denotes the vector magnitude.

Various set-theoretic measures can serve as criteria as well. Let sets S_A and S_B denote the sets of unique multi-dimensional vectors representing pixels occurring in the images A and B, respectively. Spectral composition comparison criteria can be based on methods developed for comparing the similarity and diversity of the sample sets, such as the Jaccard index [11]:

$$\uparrow JI(A,B) = \frac{|S_A \cap S_B|}{|S_A \cup S_B|} \quad \in \langle 0; 1 \rangle, \qquad (11)$$

or the Sørensen-Dice index [3]:

$$\uparrow SDI(A,B) = \frac{2\,|S_A \cap S_B|}{|S_A| + |S_B|} \quad \in \langle 0; 1 \rangle, \qquad (12)$$

where $| \, |$ denotes the cardinality of the set. Since SDI does not satisfy the triangle inequality, it can be considered a semi-metric version of JI.

Another alternative may be a modified criterion developed for texture comparison as the texture spectral composition comparison might be considered a very special case of this task. It is possible to modify the structural similarity metric (SSIM) [23] for example. SSIM compares local statistics in corresponding sliding windows in two images in either the spatial or wavelet domain. Its form consists of three terms that reflect luminance, contrast, and structure of the textures. In the case of the spectral composition comparison the structure term is irrelevant so that we define a reduced SSIM:

$$\downarrow \ rSSIM(A,B) = \frac{1}{\sharp\{r_3\}} \sum_{\forall r_3} \frac{2\mu_{A,r_3}\mu_{B,r_3}}{\mu^2_{A,r_3} + \mu^2_{B,r_3}} \frac{2\sigma_{A,r_3}\sigma_{B,r_3}}{\sigma^2_{A,r_3} + \sigma^2_{B,r_3}}, \qquad (13)$$

where $\sharp\{r_3\}$ is the spectral index cardinality, i.e., the number of spectral channels, μ_{A,r_3} is the mean of r_3 -th spectral plane of A and σ_{A,r_3} is the standard deviation of r_3 -th spectral plane of A; similarly for μ_{B,r_3} and σ_{B,r_3}. $rSSIM(A,B) = 1$ for spectrally equal textures.

A MEMD criterion was proposed in [9]

$$\downarrow \ \zeta(A,B) = \frac{1}{M} \sum_{(r_1,r_2)\in\langle A\rangle} \min_{(s_1,s_2)\in U} \left\{\rho\left(Y^A_{r_1,r_2,\bullet}, Y^B_{s_1,s_2,\bullet}\right)\right\} \qquad \geq 0, \qquad (14)$$

where $Y^A_{r_1,r_2,\bullet}$ represents the pixel at location (r_1,r_2) in the image A, $\bullet$ denotes all the corresponding spectral indices, and similarly for $Y^B_{s_1,s_2,\bullet}$. Further, ρ is an arbitrary vector metric.

3 Proposed Criterion

The proposed texture spectral similarity criterion is based on the mutual information:

$$\begin{aligned}\uparrow \ \varepsilon(A,B) = \log_2 n &- \frac{1}{n}\sum_{i=1}^{n_A} {}^A n_i \log_2 {}^A n_i - \frac{1}{n}\sum_{j=1}^{n_B} {}^B n_j \log_2 {}^B n_j \\ &+ \frac{1}{n}\sum_{i=1,j=1}^{n_A,n_B} n_{i,j}\log_2 n_{i,j} \qquad \geq 0, \qquad (15)\\ n = &\sum_{i=1,j=1}^{n_A,n_B} n_{i,j},\end{aligned}$$

where ${}^A n_i$ is the number of color x_i appearances in A, ${}^B n_j$ is the number of color y_j appearances in B, n_{ij} is the number of pixels with identical color $x_i = y_j$, and n_A, n_B are the number of the corresponding color histogram cells. $\varepsilon(A,B) = 0$ if both textures have independent colors. The criterion is non-negative and symmetric $\varepsilon(A,B) = \varepsilon(B,A)$.

3.1 Evaluation Meta-Criterion

The tested criteria are applied to quantify spectral composition differences between the template image, i.e., the first member of the degradation sequence and the remaining members. As all those sequences are created to guarantee a monotonic degradation of the original image, i.e., the similarity of the members of the sequence and the original image is decreasing with the order. A good criterion should preserve this monotonicity.

The meta-criterion is the number of monotonicity violations of the criterion τ in the experiment X:

$$\Xi^{X,\tau} = \sum_{i=1}^{l} \left[1 - \delta \left(o_i^X - o_i^{X,\tau} \right) \right] , \tag{16}$$

where τ is a tested criterion, o_i^X is the rank of a degraded image and $o_i^{X,\tau}$ its corresponding correct ordering of the τ-criterion-based ranking, and δ is the Kronecker delta function.

4 Criteria Evaluation

We proposed the set of six controllable degradation experiments described in detail below with the aim to investigate how the individual previously published (1)–(14) criteria as well as the novel proposed criterion are affected by the spectral composition changes comparing the image with its modified versions. In the following sections, we describe the performed experiments as well as used test data.

4.1 Controlled Degradation of the Test Data

A sequence of gradually degraded textural images is generated from the original test one. The original image serves as the first member of the sequence, i.e., $A_1^X = A$ and each member, except for the first one, is generated from its predecessor in the sequence as: $A_t^X = f_X \left(A_{t-1}^X \right)$, $t = 1, \ldots, l$, where l equals the length of the sequence and X is the label identifying the experiment (individual experiments described below). Further $Y_{r,t}^A$ denotes the multi-spectral pixel from the experimental image A_t^X at $r = [r_1, r_2, r_3]$ which is a multi-index with image row, column, and spectral components, respectively. X is the corresponding label of one of following six degradation experiments we established for validation tests:

A Replacing spectral intensity values of pixels with the maximal or minimal value in the used color space with the probability $p = \frac{1}{l}$:
$$Y_{r,t}^A \overset{p=\frac{1}{l}}{\longleftrightarrow} \begin{cases} [255, 255, 255]^T : \text{with } p = 0.5 \\ [0, 0, 0]^T : \text{otherwise} \end{cases}$$

B Adding a constant $c = \frac{255}{l}$ to spectral intensities of the pixels:
$$Y_{r,t}^B \overset{p}{\leftrightarrow} Y_{r,t-1}^B + [c, c, c]^T$$

C Replacing spectral intensity values of pixels with the minimal value in the used color space ($[0,0,0]^T$) with randomly driven propagating with 50% probability with 8-connected pixels from $I_r^{(8)}$:

1. $Y^C_{r,t} \overset{p}{\leftrightarrow} [0,0,0]^T$
2. $Y^C_{s,t} \overset{0.5}{=} Y^C_{r,t}, \ \forall s \in \ I_r^{(8)}$

D,E Randomly driven propagating with 50% probability with 8-connected (D) or 4-connected (E) pixels from $I_r^{(8)}$:

$$Y^D_{s,t} \overset{0.5}{=} Y^D_{r,t}, \ \forall s \in \ I_r^{(8)} / I_r^{(4)}$$

F Adding a constant $c = \frac{255}{l}$ to the spectral intensities of the pixel and randomly driven propagating with 50% probability with 8-connected pixels from $I_r^{(8)}$:

1. $Y^F_{r,t} \overset{p}{\leftrightarrow} Y^F_{r,t-1} + [c,c,c]^T$
2. $Y^F_{s,t} \overset{0.5}{=} Y^F_{r,t}, \ \forall s \in \ I_r^{(8)}$

Several selected members of the degradation sequences generated during the experiments are shown in Fig. 1.

4.2 Test Data

The proposed criterion was validated and compared with the alternative criteria on two types of visual data - color textures and BTF textures.

Color Textures. The tested criteria were validated using 250 color textures of 64 $\times$ 64 pixels saved as 24-bit RGB PNG files (Fig. 2). The textures were selected from a large collection of both natural and man-made materials. Each material category was represented by several examples. All used textures were downloaded from free internet texture databases[1,2]. The obtained results are summarized in Table 1-left.

Bidirectional Texture Functions. Simple color textures cannot represent physically correct visual appearance of the corresponding surface materials under variable observation conditions. Recent most advanced visual representation of such surfaces, Bidirectional Texture Function (BTF) [2], which is a seven-dimensional function describing surface appearance variations due to varying spatial position and illumination and viewing angles are the state-of-the-art replacement of static color textures. A static BTF texture representation requires complex seven-dimensional models, which have not yet been developed [7]. Thus,

[1] http://texturer.com/.
[2] http://www.mayang.com/textures/.

their measurement or mathematical modeling use a BTF space factorization into a large set of less dimensional factors. The measured BTF data usually consist of several thousand color images per material which are analyzed for their intrinsic dimensionality [7] and then subsequently approximated by a smaller number of BTF subspaces. It is not possible to run all experiments for all infinite number images, i.e., for any combination of the continuous spherical illumination and viewing angles, of synthetic BTF space texture components. Tested BTF measurements are represented by 20 subspace clusters, which subsequently can serve for building the BTF mathematical model. Subspace cluster were images of 32 × 32 pixels saved as 24-bit RGB PNG files. We used ten BTF data sets (one example of subspace is shown in Fig. 3) and therefore 200 textures obtained from the University of Bonn database[3] [20]. The achieved results are presented in Table 1-right.

5 Results

In this section, we present and summarize all achieved results during the experiments described in Sect. 4.1 performed on color and BTF textures and compared and comment on the performance of the criteria.

5.1 Color Textures

Achieved results of experiments with color textures in the RGB space (Fig. 2) are summarized in Table 1-left. The criterion ζ achieves the best results on average without any monotonicity violation and $\Delta_2 H$ (1) achieves the second best results, although the difference between the best criterion and the second best criterion is only 4% in average. The proposed criterion ε (15) is he third best with only 5% monotonicity violation in average. $\Delta_2 H$ is $\leq 2\%$ more correct than ε in cases **A**–**E** but 4% less correct in case of **F**. $rSSIM$ (13) is the second most correct criterion in case of **B** and **C** and its average error is 6% but worsen it performance in cases **D** and **E**. Other criteria fail on average more than 15% and cannot be considered reliable, although in some cases they work well, e.g., ΔGCM_{00}^{111} in case of **F**, ΔH, $\Delta_{1/2} H$, $\cap H$, d_{sc}, d_{can}, χ^2 in case of **A**. The criteria were on average the most successful in case of **A** with average failure only 4% and the least successful in case of **F** with average failure 53%.

5.2 Bidirectional Texture Functions

The achieved results are summarized in the right part of Table 1. Both criteria ε and ζ are the only criteria that reached zero average error in all experiments. The second most successful criterion $\Delta_2 H$ achieved 1% worse result in average. The ε, ζ can be considered as absolutely reliable for BTF textures. $rSSIM$ achieved 5% average error and it is quite successful in most experiments but

[3] http://cg.cs.uni-bonn.de/en/projects/btfdbb/download/ubo2003/.

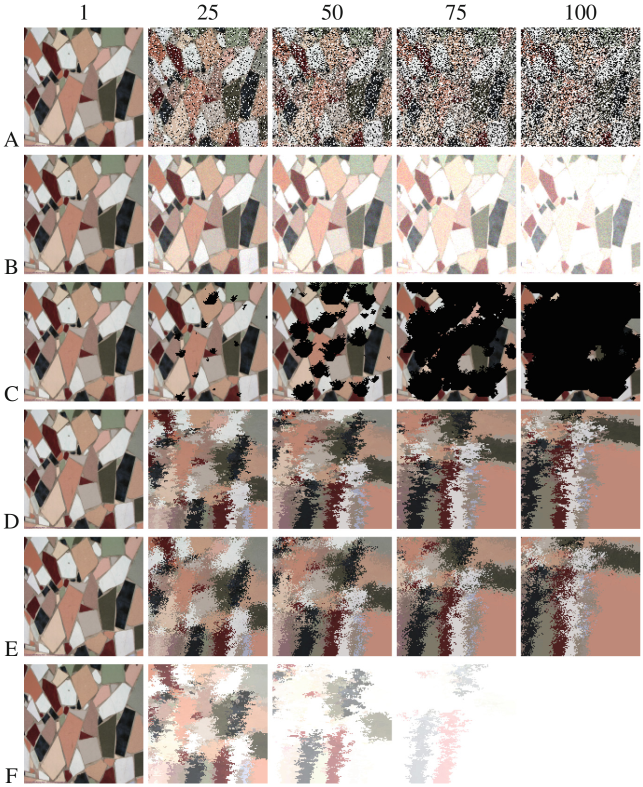

Fig. 1. The figure illustrates selected members of the degradation sequence generated during the experiments, **A**-**F** top-down. The leftmost column represents the original image, and the degradation intensifies in the rightward direction, where the column number indicates the order of the image in the sequence.

Fig. 2. Selected examples of the color textures used in our experiments.

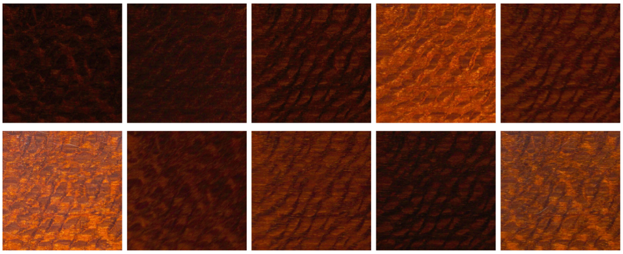

Fig. 3. Textures representing BTF subspace clusters approximating original BTF data acquired by measuring the wood material. Original data were taken from BTF database of the University of Bonn [20]. BTF subspace textures were used in our experiments.

Table 1. The average strict monotonicity violation (in percent) for 250 test color texture sequences (left) 200 test BTF data sequences (right) per experiment performed in the RGB color space, average over all experiments and the rank for the tested criteria.

Color textures									BTF textures							
	A	B	C	D	E	F	$\oslash$	Rank	A	B	C	D	E	F	$\oslash$	Rank
ΔH	0	14	14	35	22	86	29	9	0	3	3	0	1	67	12	5
$\Delta_2 H$	0	7	7	2	2	7	4	2	0	1	1	0	0	3	1	2
$\Delta_\infty H$	5	12	12	97	97	98	54	14	1	4	4	96	96	98	50	10
$\Delta_{1/2} H$	0	31	31	49	48	9	28	8	0	18	18	73	70	6	31	9
$\cap H$	0	14	14	35	22	86	29	9	0	3	3	0	1	67	12	5
d_{sc}	0	16	16	3	3	86	21	6	0	3	3	0	0	64	12	5
d_{can}	0	33	33	29	28	55	30	10	0	20	20	23	23	8	16	6
KL	19	37	36	20	23	86	37	12	18	32	32	17	20	65	31	9
J	19	38	38	4	4	86	32	11	17	32	32	1	1	65	25	8
χ^2	0	16	16	4	4	86	21	6	0	3	3	1	1	64	12	5
ΔGCM_{00}^{111}	14	13	13	23	24	0	15	5	4	4	4	23	24	0	10	4
d_{cos}	13	13	13	43	43	20	24	7	2	2	2	45	46	37	22	7
JI	1	31	31	54	49	98	44	13	0	16	16	0	0	98	22	7
SDI	1	32	32	54	49	98	44	13	0	17	17	0	0	98	22	7
$rSSIM$	3	3	3	12	13	3	6	4	0	0	0	13	14	1	5	3
ζ	0	0	0	0	0	0	0	1	0	0	0	0	0	0	0	1
ε	1	9	9	3	4	3	5	3	0	0	0	0	0	0	0	1
$\oslash$	4	19	19	27	26	53	25		2	9	9	17	17	44	17	

Table 2. The average evaluation time, on Pentium-2.8 GHz-equivalent CPU, depending on the size of compared images for individual criteria.

	8×8	16×16	32×32	64×64
ΔH, $\cap H$, d_{sc}, d_{can}, J, χ^2	0.7 s	0.7 s	0.7 s	0.7 s
EMD	1.8 ms	85.6 ms	5.7 s	7.6 min
ΔGCM_{00}^{111}	67.0 µs	0.1 ms	0.2 ms	0.5 ms
d_{cos}	32.0 µs	88.0 µs	93.0 µs	0.6 ms
JI, SDI	0.3 ms	4.0 ms	9.0 ms	48.0 ms
$rSSIM$	31.0 µ s	0.1 ms	0.2 ms	1.4 ms
ζ	0.1 ms	2.0 ms	18.0 ms	0.2 s
ε	0.1 ms	0.2 ms	0.7 ms	2.2 ms

it fails again in cases **D** and **E**. ΔGCM_{00}^{111} achieved better results like the other criteria in **A**–**C** but its average error in case of **D** and **E** stayed the same. In average, all criteria, except $\Delta_{1/2}H$, achieved better results (with average improvement 8%), which may be due to the lower amount of distinct colors of BTF textures compared to the data described in Sect. 4.2.

6 Conclusions

We introduced the mutual information based criterion for comparing the spectral similarity of the color textures and bidirectional texture functions. Although the criterion neglects spatial pixels arrangement and thus it represents only a partial solution for the quality assessment of the multi-spectral textured images and also for the most advanced visual representation of material surfaces - the bidirectional texture function, it can assist in numerous texture-analytic or synthesis applications. The performance quality of the proposed criterion is demonstrated on the extensive series of specially designed monotonically image degrading experiments, which also serve for the comparison with the existing alternative methods.

Similarly to several other existing approaches (1)–(8), the criterion (15) is based on 3-D histograms, thus it cannot be efficiently used for hyperspectral images. Although it has slightly worse performance than the best ζ (14) spectral similarity criterion, it is symmetric, can be easily modified to a metric, and is much faster.

The presented criterion proposes a reliable fully automatic alternative to psychophysical experiments, which are, moreover, extremely impractical due to their cost and strict demands on design setup, conditions control, human resources, and time.

Acknowledgments. The Czech Science Foundation project GAČR 19-12340S supported this research.

References

1. Cuturi, M., Peyré, G.: A smoothed dual approach for variational wasserstein problems. SIAM J. Imaging Sci. **9**(1), 320–343 (2016)
2. Dana, K.J., Nayar, S.K., van Ginneken, B., Koenderink, J.J.: Reflectance and texture of real-world surfaces. In: CVPR, pp. 151–157. IEEE Computer Society (1997)
3. Dice, L.R.: Measures of the amount of ecologic association between species. Ecology **26**(3), 297–302 (1945)
4. Galloway, M.: Texture analysis using gray level run lengths. Comput. Graph. Image Process. **4**(2), 172–179 (1975)
5. Haindl, M., Kudělka, M.: Texture fidelity benchmark. In: 2014 International Workshop on Computational Intelligence for Multimedia Understanding (IWCIM), pp. 1–5. IEEE Computer Society CPS, Los Alamitos, November 2014. https://doi.org/10.1109/IWCIM.2014.7008812, http://ieeexplore.ieee.org/stamp/stamp.jsp?tp=&arnumber=7008812&isnumber=7008791
6. Haindl, M., Mikeš, S.: Unsupervised texture segmentation using multispectral modelling approach. In: Tang, Y., Wang, S., Yeung, D., Yan, H., Lorette, G. (eds.) Proceedings of the 18th International Conference on Pattern Recognition, ICPR 2006. vol. II, pp. 203–206. IEEE Computer Society, Los Alamitos, August 2006. https://doi.org/10.1109/ICPR.2006.1148
7. Haindl, M., Filip, J.: Visual Texture. Advances in Computer Vision and Pattern Recognition. Springer, London (2012). https://doi.org/10.1007/978-1-4471-4902-6
8. Haralick, R.M., Shanmugam, K., Dinstein, I.: Textural features for image classification. IEEE Trans. Syst. Man Cybern. **3**(6), 610–621 (1973)
9. Havlíček, M., Haindl, M.: Texture spectral similarity criteria. IET Image Process. **13** (2019). https://doi.org/10.1049/iet-ipr.2019.0250
10. Howarth, P., Rüger, S.: Fractional distance measures for content-based image retrieval. In: Losada, D.E., Fernández-Luna, J.M. (eds.) ECIR 2005. LNCS, vol. 3408, pp. 447–456. Springer, Heidelberg (2005). https://doi.org/10.1007/978-3-540-31865-1_32
11. Jaccard, P.: Etude comparative de la distribution florale dans une portion des Alpes et du Jura. Impr. Corbaz (1901)
12. Kokare, M., Chatterji, B., Biswas, P.: Comparison of similarity metrics for texture image retrieval. In: TENCON 2003. Conference on Convergent Technologies for the Asia-Pacific Region, vol. 2, pp. 571–575. IEEE (2003)
13. Kudělka, M., Haindl, M.: Texture fidelity criterion. In: 2016 IEEE International Conference on Image Processing (ICIP), pp. 2062–2066. IEEE, September 2016. https://doi.org/10.1109/ICIP.2016.7532721, http://2016.ieeeicip.org/
14. Laws, K.: Rapid texture identification. In: Proceedings of SPIE Conference on Image Processing for Missile Guidance, pp. 376–380 (1980)
15. Manjunath, B.S., Ma, W.Y.: Texture features for browsing and retrieval of image data. IEEE Trans. Pattern Anal. Mach. Intell. **18**(8), 837–842 (1996). https://doi.org/10.1109/34.531803
16. Mindru, F., Moons, T., Van Gool, L.: Color-based moment invariants for viewpoint and illumination independent recognition of planar color patterns. In: Singh, S. (ed.) International Conference on Advances in Pattern Recognition, pp. 113–122. Springer, London (1998). https://doi.org/10.1007/978-1-4471-0833-7_12
17. Ojala, T., Pietikäinen, M., Mäenpää, T.: Multiresolution gray-scale and rotation invariant texture classification with local binary patterns. IEEE Trans. Pattern Anal. Mach. Intell **24**(7), 971–987 (2002)

18. Puzicha, J., Hofmann, T., Buhmann, J.M.: Non-parametric similarity measures for unsupervised texture segmentation and image retrieval. In: Proceedings of the IEEE International Conference on Computer Vision and Pattern Recognition, pp. 267–272. IEEE (1997)
19. Rubner, Y., Tomasi, C., Guibas, L.J.: The earth mover's distance as a metric for image retrieval. Int. J. Comput. Vis. **40**(2), 99–121 (2000). https://doi.org/10.1023/A:1026543900054
20. Sattler, M., Sarlette, R., Klein, R.: Efficient and realistic visualization of cloth. In: Eurographics Symposium on Rendering 2003, June 2003
21. Swain, M.J., Ballard, D.H.: Color indexing. Int. J. Comput. Vis. **7**(1), 11–32 (1991)
22. Viethen, J., van Vessem, T., Goudbeek, M., Krahmer, E.: Color in reference production: the role of color similarity and color codability. Cogn. Sci. **41**, 1493–1514 (2017)
23. Wang, Z., Bovik, A.C., Sheikh, H.R., Simoncelli, E.P.: Image quality assessment: from error visibility to structural similarity. IEEE Trans. Image Process. **13**(4), 600–612 (2004). https://doi.org/10.1109/TIP.2003.819861
24. Wang, Z., Simoncelli, E.P.: Translation insensitive image similarity in complex wavelet domain. In: IEEE International Conference on Acoustics, Speech, and Signal Processing, 2005. Proceedings. (ICASSP 05), pp. 573–576 (2005)
25. Yuan, J., Wang, D., Cheriyadat, A.M.: Factorization-based texture segmentation. IEEE Trans. Image Process. **24**(11), 3488–3497 (2015). https://doi.org/10.1109/TIP.2015.2446948
26. Zhang, D., Lu, G.: Evaluation of similarity measurement for image retrieval. In: Proceedings of the 2003 International Conference on Neural Networks and Signal Processing, 2003, vol. 2, pp. 928–931. IEEE (2003)
27. Zujovic, J., Pappas, T., Neuhoff, D.: Structural texture similarity metrics for image analysis and retrieval. IEEE Trans. Image Process. **22**(7), 2545–2558 (2013). https://doi.org/10.1109/TIP.2013.2251645